MIMO Distributed Imaging of Rotating Targets for Improved 2D Resolution

D. Pastina, F. Santi, M. Bucciarelli

***Abstract*—This paper deals with MIMO distributed radar imaging of rotating targets. The distributed system is based on formation flying platforms, which can be configured with proper cross-track and along-track displacements. The platforms carry active radar systems transmitting almost orthogonal waveforms; exploiting both monostatic and bistatic acquisitions, range and cross-range resolution improvement can be achieved and a maximum theoretical 2D resolution cell improvement factor can be obtained significantly greater than the number of flying platforms. The required distributed focusing technique is developed and its effectiveness and robustness is tested against simulated data. The proposed distributed system could be suitable to the application of ship target imaging using a reconfigurable formation of platforms for maritime surveillance in wide sea areas.**

***Index Terms*—ISAR, SAR, MIMO, Resolution.**

I. Introduction

In recent years the scientific community has devoted considerable attention to the study of networks of low-mass and low-cost jointly operating sensors. Well known advantages are the robustness to out of services and the reconfiguration capability of the overall system, thus enabling many different applications, [1]. Moreover, despite the poor performance of each sensor in the network and the synchronization issues, [2], the possibility of achieving comparable or even better performance with respect to single sensor (SS) systems has been widely addressed.

High resolutions are typically required in radar images of man-made targets (such as ships). As well known, the range resolution (r.r.) of a Synthetic Aperture Radar (SAR) image depends on the transmitted bandwidth, which can be limited if a low-cost and low-mass sensor is considered or more in general is limited by regulation constraints. In [3], a technique was proposed to improve the r.r. of a SAR image by exploiting multiple surveys of the same area, see also [4]-[5]. The joint processing of the multiple-surveys acquired signals could result in an overall synthetic bandwidth greater than the transmitted one: an improvement of r.r. up to the number of surveys could be achieved selecting proper acquisition geometries. The concept was generalized in [6] for a Multiple-Input-Multiple-Output (MIMO) SAR system able to exploit both monostatic and bistatic acquisitions to allow a maximum theoretical improvement factor greater than the number of operating systems, [7].

While the r.r. depends on the transmitted bandwidth, the cross-range resolution (c.r.r.) depends on the processed synthetic aperture: specifically in Inverse SAR (ISAR) it is due to the motion of the target itself, [8]. Therefore, depending on the particular conditions, the achievable c.r.r. could be poor. To counteract this effect the Distributed ISAR technique was proposed in [9]: exploiting signals received from a formation of properly spaced sensors, a wider observation angle than in the SS case is emulated. The achieved c.r.r. improvement is equal or even higher to the number of sensors in the multistatic and MIMO case respectively.

In this paper a constellation of imaging systems is considered in order to produce images of man-made rotating targets with increased r.r and c.r.r. when compared to SS conventional low-medium resolution images. In particular, generalizing the MIMO SAR concept in [6] and MIMO ISAR in [9], a 2D-MIMO SAR/ISAR system is proposed based on a formation of platforms which can be configured with proper cross-track and along-track displacements. A maximum theoretical 2D resolution cell improvement factor can be achieved significantly greater than the number of flying platforms, by jointly exploiting both the monostatic and the bistatic acquisitions. Obviously this requires that the imaged scatterers have constant reflectivity for all the exploited observations. This hypothesis can be regarded as reasonable in our case since we are focusing on cases implying quite limited changes of the observation angle over the different acquisitions (i.e. low-medium resolution, requiring at most few degrees) so that the target can be assumed in the pseudo-monostatic region (angular differences less than 5°). Some preliminary results concerning the proposed 2D-MIMO SAR/ISAR were presented in [10]. In this paper the concept is derived for more general configurations of systems and signal model; an enhanced and more complete focusing technique (with respect to the one proposed in [10]) is presented able not only to improve the resolution of isolated scatterers but also to resolve very close

This paragraph of the first footnote will contain the date on which you submitted your paper for review. It will also contain support information, including sponsor and financial support acknowledgment. For example, "This work was supported in part by the U.S. Department of Commerce under Grant BS123456".

Debora Pastina is with the DIET dept. of the University of Rome "La Sapienza", Rome, Italy (e-mail: debora@infocom.uniroma1.it).

Fabrizio Santi is with the DIET dept. of the University of Rome "La Sapienza", Rome, Italy (e-mail: santi@die.uniroma1.it).

Marta Bucciarelli is with the DIET dept. of the University of Rome "La Sapienza", Rome, Italy (e-mail: mbucciarelli@infocom.uniroma1.it).

scatterers not separable in the SS case. New case studies are considered to show the achievable performance and highlight the robustness to the presence of perturbations in the exploited formation of systems and in the considered rotation motion of the target.

The 2D-MIMO SAR/ISAR system concept mainly addresses those applications, where the resolution requirements can change with the specific operational conditions. An example is maritime surveillance where the coherent processing interval (CPI) for image formation can be limited by the constraint of keeping fixed the ship rotation axis: in such a case, depending on the specific conditions, SS techniques can provide images with low c.r.r.. Even when c.r.r. is acceptable it could be of interest to enhance it without requiring longer integration times. Moreover depending on the value of the angle between the radar Line Of Sight (LOS) and the ship target centerline, it could be of interest to improve resolution in range or in cross-range or in both directions. In this context the 2D-MIMO SAR/ISAR concept fosters the flexible use of a formation in supporting the complete control, surveillance and monitoring in wide sea areas.

The paper is organized as follows: after introducing the 2D-MIMO SAR/ISAR concept in Section II, the required focusing technique is described in Section III while Section IV reports results obtained against simulated case studies and analyzes the robustness of the achievable performance. Finally some conclusions are drawn in Section V.

II. 2D MIMO SAR-ISAR CONCEPT

The operative scenario comprises a formation of S air - or space - platforms. Each platform is equipped with an active radar system, able to receive and separate echoes from the different transmissions through the use of almost orthogonal waveforms and having its antenna steered towards the target to be imaged. The position of each platform in the XYZ reference system is described according to a couple of angles, namely aspect angle ϕ_i and off-nadir angle θ_i for i=1,..., S. This is a generalization with respect to [10], where angular constraints leaded to a symmetric formation of platforms. If we consider the h-th transmitting platform and l-th receiving platform (h,l=1,..., S) we can define the n-th equivalent sensor position (n=1,…, N): it is a real position in the case of a monostatic acquisition, i.e. couple (h,h), and a fictitious position for a bistatic couple (h,l) with $h \neq l$. Therefore we consider a formation of equivalent sensors characterized by different off-nadir angles $\vartheta_n=(\theta_h + \theta_l)/2$ and azimuth angles $\varphi_n=(\phi_h + \phi_l)/2$.

Signals received by all the equivalent sensors can be properly processed in order to produce an improved image. This image can be thought as equivalent to the one achievable if processing the signal received by fictitious monostatic sensor with reference aspect and off-nadir angle equal to ϕ_0 and θ_0 respectively, transmitting a wider bandwidth and acquiring for a longer time with respect to the real systems in the formation. The demodulation of the signals received from each sensor with respect to the common reference results in a relative spectral shift between the different equivalent sensors, [6]. The spectral

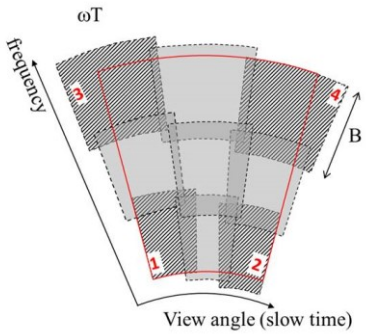

Figure 1. 2D-MIMO SAR/ISAR data grids.

shift of the n-th equivalent sensor is:

$$\Delta f_n \cong f_c(\vartheta_n - \theta_0)/\tan(\theta_0) \quad (1)$$

being f_c the carrier frequency. It is worth noticing that the spectral shift in (1) is defined with respect to scene center; this shift can vary with changing the position inside the imaged scene as a consequence of variation of the local incidence angle. Differently from [10], where local variations were neglected, this characteristic is here properly taken into account in the derivation of the 2D-MIMO focusing technique.

The target is modeled as a rigid body consisting of K scatterers. In this paper we focus on target rotation assuming the translation negligible or already compensated, [8]. Moreover we also assume the integration time T suitable for image formation already selected, [11], [12], and limited to some specific value. In first approximation the target is supposed to undergo a 1D rotation around the Z axis with a rotation rate equal to ω. This induces a linear angular shift in the time aperture, [9], equal to

$$\zeta_n^k(t) = \zeta_0^k - \varphi_n + \omega(t - t_0) \quad (2)$$

where ζ_0^k is the aspect of the k-th scatterer as observed from the reference aspect ϕ_0.

Based on (1) and (2), the data corresponding to the different sensors are displaced in the polar plane (range frequency & view angle) as shown in Fig. 1 for the case S=4. It is possible to identify N = 9 different acquisitions ([7]), the striped ones monostatic while the gray ones bistatic, partially overlapped both in the range frequency and in the view angle domain.

Looking at Fig. 1, since $(\phi_1,\phi_3) \leq \phi_0 \leq (\phi_2,\phi_4)$ and $(\theta_1,\theta_2) \leq \theta_0 \leq (\theta_3,\theta_4)$, it is evident that by coherently processing the data portion identified by the red box it is possible to obtain a r.r. and a c.r.r. improvement factor γ_r and γ_{cr} equal to:

$$\gamma_r = 1 + \frac{[\min(\theta_0-\theta_1,\theta_0-\theta_2)-\max(\theta_0-\theta_3,\theta_0-\theta_4)]}{B\tan(\theta_0)}$$
$$\gamma_{cr} = 1 + \frac{[\min(\phi_0-\phi_1,\phi_0-\phi_3)-\max(\phi_0-\phi_2,\phi_0-\phi_4)]}{\omega T} \quad (3)$$

where B is the bandwidth of the transmitted waveform.

From (3) we observe that the highest improvement is achieved when the platforms are symmetrically displaced ($\phi_1=\phi_3$, $\phi_2=\phi_4$, $\theta_1=\theta_2$, $\theta_3=\theta_4$) and maximally spaced (in angle) still assuring a continuous coverage in range frequency and view angle (i.e. no gaps or overlaps in the polar domain). In this case $\gamma_r=\gamma_{cr}=3$ for the case S=4 and a global improvement factor equal to $\gamma=\gamma_r\cdot\gamma_{cr}= 9$ is obtained for the 2D cell area.

III. 2D-MIMO SAR-ISAR Focusing Technique

To achieve an image with improved range and cross-range resolutions a 2D processing technique is required. The proposed approach is a decentralized technique for multi-angle SAR/ISAR focusing, based on a modified version of the Polar Format Algorithm (PFA, [13]). This decentralized approach (Fig. 2a) first focuses and then coherently combines N low resolution ISAR images to achieve the high resolution image.

For each branch in the scheme the processing is organized as follows: 1) Fast-time compression; 2) Modified Polar to Cartesian interpolation to remove from SS data the range and Doppler migration, co-register the N low-resolution images and scale the axes as all the acquisitions were monostatic; 3) Range profile formation; 4) Slow-time Fourier transform.

At this point the low resolution SS ISAR images LR_n for n=1,..., N are obtained as intermediate output. The following steps refer specifically to the processing of the multi-sensor data: a) Azimuth distributed processing (here named MIMO-ISAR, following nomenclature in [9]), which provides M high c.r.r. images, each one achieved by means of the appropriate combination of a subset of the N low resolution images; b) Range distributed processing (here named MIMO-SAR, following nomenclature in [6]), which properly combines the M high c.r.r. images to yield the final high resolution image.

The proposed technique guarantees a space-invariant point spread function (PSF) also in the case of non-symmetric acquisition geometries differently from the technique in [10] which represents a limit case, where M is always equal to 3 due to the specific symmetry of the acquisition geometry.

The MIMO ISAR processing is detailed in Fig. 2b. If the total frequency extent is divided in M intervals, then the goal of azimuth processing is to obtain M high c.r.r. images HCR_m for m=1,...,M, by separately processing M groups of images LR_n, selected in the "Low resolution image and data selection" step. In the case N=9 each group is always formed by 3 images (a, b and c); they correspond to raw data filling an angular portion of the polar support in Fig. 1 pertaining to a specific range frequency interval, whose central value is relative to a specific off-nadir angle. After compensating the constant phase term depending on the distance between the sensor and the target fulcrum, signals are time shifted in order to synthesize an overall CPI equal to $\gamma_{cr} \cdot T$. Since local variations of the off-nadir angle, inside the imaged scene and with the considered sensor, can cause abrupt slow time phase changes, an azimuth phase junction step is applied to each cross-range cell, differently from [10]. To this purpose for each cross-range cell the corresponding sub-image is obtained by selecting a proper strip centered on the cross-range cell under test (CUT). For each range bin the phase compensation term of sensor a(c) with respect to reference b is extracted from the scalar product between sub-image a(c) and b. After phase compensation only the cross-range CUT is retained. The azimuth phase junction procedure is repeated for all cross-range cells, then time selection is applied and finally the images are coherently combined. Analytical details relating the time selection step and the target motion can be found in [9] and in [14]. Here we observe that time selection is needed when the observations from the different sensors are partially overlapped leading to a γ_{cr} value lower than the maximum theoretical bound (3 in our case). However a partial overlap is needed when applying the phase junction step to achieve a PSF with desired characteristics. Therefore there is an implicit trade-off between resolution gain and quality of the final image. From our experience 10-20% overlap would suffice, thus allowing γ_{cr}=2.8-2.6. The M high c.r.r. images from the MIMO ISAR distributed processing feed the subsequent MIMO SAR sketched in Fig. 2c. The chain is composed by the cascade of three main steps: a range phase junction stage, a frequency selection stage and a coherent combination stage. The MIMO SAR processing performs similarly to MIMO ISAR but works in range direction: almost the same considerations apply. At the output of the range distributed processing the final high r.r. and c.r.r. image is obtained. It is worth noticing that the MIMO ISAR or the MIMO SAR processing could be bypassed achieving images with single dimension resolution improvement.

IV. Simulated Performance Analysis

To test the proposed technique we simulated the case of S=4 X-band (f_c=10 GHz) space-borne (R_0=850 km and θ_0=60°) radar systems observing a moving target. While in [10] we considered a set of isolated scatterers proving only the resolution improvement capabilities, in this paper we account for sets of interfering and isolated scatterers, proving also the separation capabilities. Moreover, while in a first set of cases (Fig. 3 to Fig. 5) we simulate the target motion as a rotation

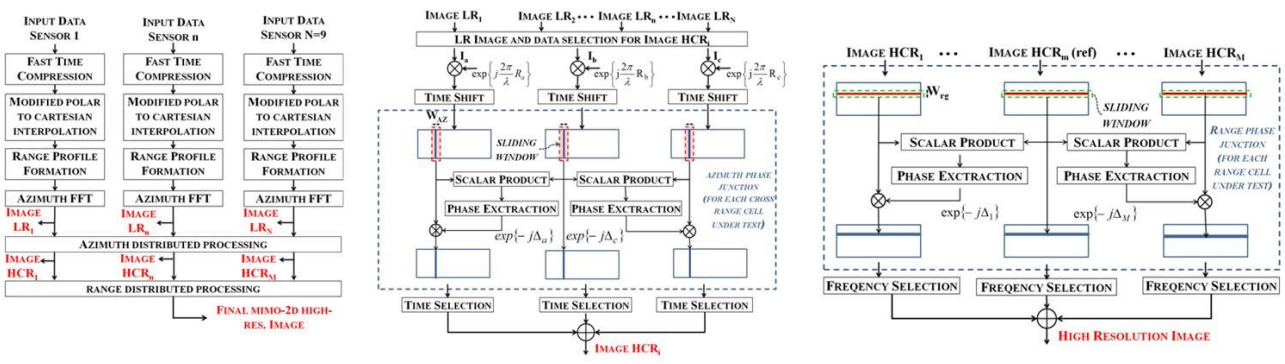

Figure 2. 2D-MIMO SAR/ISAR processing scheme: (a) general block scheme, (b) MIMO ISAR processing, (c) MIMO SAR processing.

with constant rate ω (0.4°/sec) around the Z axis as done in [10], the technique is also validated for target undergoing 3D motion (Fig. 6). In all cases a set of almost orthogonal up-down chirped waveforms is used ([9], [15]-[16]) thus causing a limited degradation due to a floor of not compressed residual signal. As discussed in [6] strategies based on separation in the slow time or Doppler domain could be applied to obtain fully orthogonal waveforms. However it is worth noticing that the coherent integration gain provided by the MIMO-2D allows a further mitigation of the effects of the not compressed floor. It is worth noticing that all the results reported in the following were obtained assuming the imaged scatterers as ideal point scatterers with constant reflectivity for all the exploited observations. As stated in Section I this assumption is reasonable taking into consideration the limited changes in the view angle entailed by all the considered cases. A moderate degradation of the image quality is expected if the operative conditions do not comply with these assumptions.

First of all an analysis of the achievable PSFs has been conducted. Referring to a symmetric configuration ($\theta_1=\theta_2=59.20°$, $\theta_3=\theta_4=60.80°$, $\phi_1=\phi_3=-0.57°$, $\phi_2=\phi_4=0.57°$) Fig. 3a and b show respectively the cross-range and range PSFs compared to the SS conventional PSF; the MIMO-2D PSF achievable if the considered waveforms were perfectly orthogonal (labeled as MIMO-2D$_{ideal}$) is also reported for comparison. As it is apparent from Fig. 3a-b the MIMO-2D allows an improvement in both the c.r.r. and r.r.. In particular we obtain a c.r.r. of 1.2 m in the SS (T=1.8 sec) and MIMO-SAR cases and of 0.46 m in the MIMO-ISAR and MIMO-2D cases. On the other hand a r.r. of about 1.5 m is achieved in the SS (B=100 MHz) and MIMO-ISAR cases and of about 0.58 m in the MIMO-SAR and MIMO-2D cases. Specifically we obtain the improvement factors $\gamma_r=2.60$, $\gamma_{cr}=2.59$ and $\gamma=6.74$. We point out that in both frequency and view angle domains overlaps have been considered ($\eta_f=\Delta f/B=0.8$ and $\eta_T=|\phi_1|/(\omega T)=0.79$). Results in Fig. 3a-b confirm our previous observations on the limited impact in using not perfectly orthogonal waveforms.

Moving to non-symmetric configurations (geometry 1: $\phi_1=-0.63°$, $\phi_2=0.46°$, $\phi_3=-0.51$, $\phi_4=0.57°$, $\theta_1=59.12°$, $\theta_2=59.29°$, $\theta_3=60.63°$, $\theta_4=60.79°$; geometry 2: $\phi_1=-0.51°$, $\phi_2=0.34°$, $\phi_3=-0.46°$, $\phi_4=0.57°$, $\theta_1=59.29°$, $\theta_2=59.44°$, $\theta_3=60.71°$, $\theta_4=60.56°$) a decrease is observed both in cross and slant range, Fig. 3c-d, in terms of achievable resolution improvement factors. Specifically as predicted by the theory, $\gamma_r=2.35$, $\gamma_{cr}=2.35$ and $\gamma=5.52$ for the geometry 1 case and $\gamma_r=2.12$, $\gamma_{cr}=2.11$ and $\gamma=4.47$ for the geometry 2 case. However this result doesn't mean performance degradation with respect to the more efficient symmetric formation case, since the technique reaches the best achievable result with the considered acquisition geometries.

Cases of extended targets are then considered. Fig. 4 shows the image of a grid of point-like scatterers, with the same parameters of the Fig. 3a-b. Two clusters of four scatterers are placed at distances such that they cannot be separated with the conventional SS technique, Fig. 4a (being white "×" the true scatterers positions); moving to the 2D-MIMO case, Fig. 4b, both c.r.r. and r.r. improve allowing us to separate the four different scattering centers as confirmed by the inspection of the cross range and range cuts (also for MIMO-ISAR and SAR) of the scatterers around the scene center in Fig. 4c-d. A more complex target is considered in Fig. 5 showing a ship with length about 120 m and different levels of superstructure. In this case B=33.3 MHz and T=0.6 s have been considered being the remaining parameters as above. For such case we have a r.r. of 4.5 m in the SS case and 1.75 m in the 2D-MIMO, while in the cross-range we move from 3.58 m to 1.38 m. As the resolution increases scattering centers not resolvable with SS (Fig. 5a) can be resolved via MIMO-2D (Fig. 5b).

The hypothesis of 1D uniform rotation is then removed considering a target undergoing 3D motion with sinusoidal yaw, pitch and roll in addition to the uniform rate ω, with amplitude and frequency equal to $A_{yaw}=0.1°$, $f_{yaw}=0.2$ Hz, $A_{pitch}=0.1°$, $f_{pitch}=0.18$ Hz, $A_{roll}=0.5°$ and $f_{roll}=0.09$ Hz. Since 3D rotation motion impacts on the cross-range/Doppler domain as

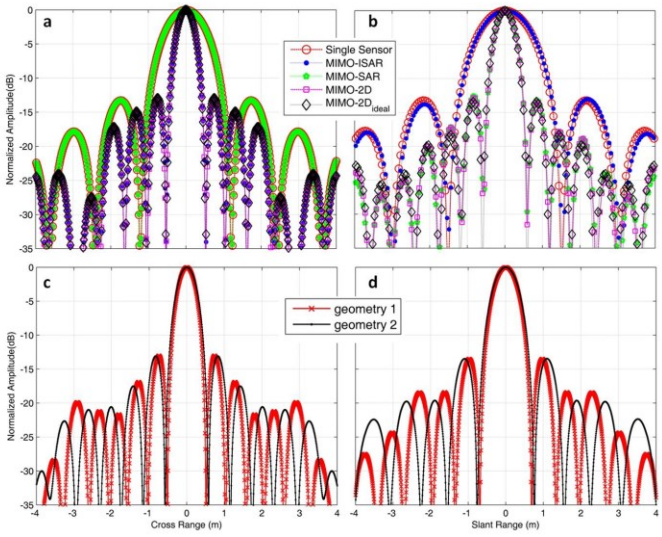

Figure 3. PSF analysis: (a) cross range and (b) slant range cuts for symmetric acquisition geometry, (c) cross range and (d) slant range cuts for asymmetric acquisition geometries.

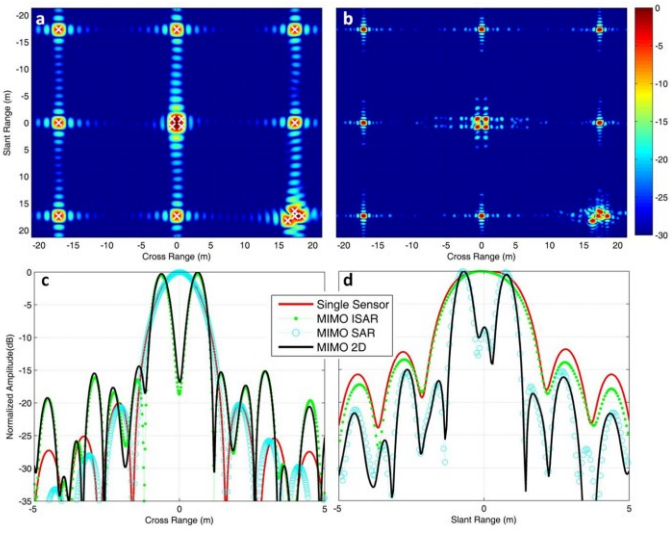

Figure 4. Grid of point-like scatterers: (a) Single sensor, (b) 2D MIMO images; (c) cross-range and (d) slant range cuts comparison.

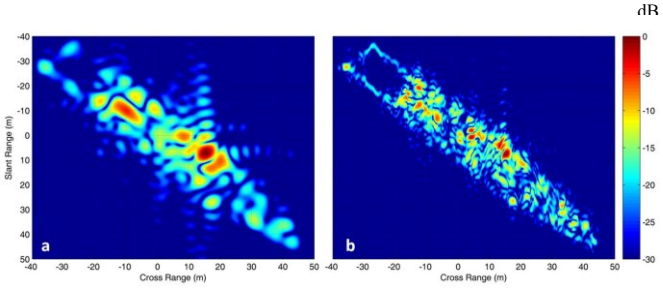

Figure 5. Ship target model – (a) Single sensor, (b) 2D MIMO images.

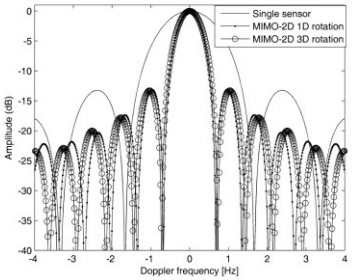

Figure 6. Comparison of Doppler PSF in presence of 1D and 3D motion.

being superstructure scatterers the most sensitive to pitch and roll motions, [11], Fig. 6 shows the Doppler PSF for the scatterer representing the apex of the mainmast of the above target. In this case MIMO-2D focusing technique has been applied matching the parameters to the vertical component of the motion orthogonal to the horizontal plane comprising the LOS, [14], and the PSFs have been centered on the same Doppler frequency value to allow the comparison. Results achievable in the same conditions but setting to zero pitch and roll are also shown. We notice a similar output for the 3D and 1D rotation motions, the slight difference in resolution gain due to the fact that not only yaw, but also pitch and roll contribute to the vertical component of the motion.

Finally we analyze the technique robustness in presence of disturbances causing deviations of the actual acquisition geometry with respect to the nominal geometry. Particularly we consider the position of each platform in the XYZ reference system as a random variable uniformly distributed in a sphere, with center on the nominal position and radius ρ. Different platforms are affected by independent perturbations. The performance robustness is investigated by analyzing the mean value (100 independent trials) of resolution and sidelobe level (in dB) of range and cross-range PSFs achieved by matching the focusing to the nominal geometry. Setting ρ=5 km the resolution improvement is basically maintained under non ideal conditions (theoretical r.r. and c.r.r. ΔR=0.58 m and ΔCR=0.46 m respectively, achieved r.r. and c.r.r. ΔR=0.60 m and ΔCR=0.47 m), while a small degradation is observed for the Side Lobe Ratio (-12.94 and -13.07 in range and cross range respectively). This robustness is obviously also a consequence of: (i) spaceborne geometry limiting the perturbations on the off-nadir and aspect angles even in presence of not negligible perturbations on the positions (tighter requirements expected in the airborne case); (ii) overlap between the acquisitions in the polar plane; (iii) presence of the phase junction step able to counteract the effect of disturbances inducing phase discontinuities.

V. Conclusions

In this paper a technique has been proposed to jointly increase the r.r. and c.r.r. of radar images of rotating targets. A 2D-MIMO SAR/ISAR system has been configured, consisting in a formation of platforms with proper cross-track and along-track displacements, each carrying an active radar system. A distributed focusing technique for the joint elaboration of the monostatic and bistatic acquired data has been developed and tested against simulated data. Results show that the achievable images can have a 2D resolution cell improved of a factor up to 9 when a formation of four platforms is considered. The flexible use of such a constellation of platforms could allow the improvement of resolution in range or cross-range or in both directions on the basis of the specific needs and could be useful for example for non-cooperative ship target imaging.

Acknowledgment

The authors acknowledge fruitful discussions with Prof. P. Lombardo of University of Rome "La Sapienza".

References

[1] G. Krieger, A. Moreira, "Spaceborne bi- and multistatic SAR: potential and challenges", *IEE Proceedings - Radar, Sonar and Navigation*, vol. 153, Issue 3, pp. 184 – 198, June 2006.

[2] M. Younis, R. Metzig, G. Krieger, "Performance prediction of a phase synchronization link for bistatic SAR", *IEEE Geosci. Remote Sens. Letters*, vol. 3, no. 3, pp. 429-433, July 2006.

[3] C. Prati, R. Rocca, "Improving Slant-Range Resolution With Multiple SAR Surveys", *IEEE Trans. on AES*, 1993, 29, (1), pp. 135-144.

[4] G. Fornaro, V. Pascazio, G. Schirinzi, "Resolution Improvement Via Multipass SAR Imaging", *Proc. of IGARSS*, Sydney (AUS), July 2001.

[5] S. Guillaso, A. Reigber, L. Ferro-Famil, E. Pottier, "Range Resolution Improvement of Airborne SAR Images", *IEEE Geosci. Remote Sens. Letters*, 2006, 3, (1), pp. 135-139.

[6] D. Cristallini, D. Pastina, P. Lombardo, "Exploiting MIMO SAR Potentialities with Efficient Cross-Track Constellation Configurations for Improved Range Resolution", *IEEE Trans. on GRS*, Vol. 49, Issue 1, January 2011, pp. 38-52.

[7] B. Correll, "Efficient Spotlight SAR MIMO Linear Collection Geometries", *Proc. EuRAD*, Amsterdam (NL), Oct. 2008.

[8] D.R. Wehner, *High-Resoultion Radar*, Artech House, Boston, 1995.

[9] D. Pastina, M. Bucciarelli, P. Lombardo, "Multistatic and MIMO Distributed ISAR for Enhanced Cross-Range Resolution of Rotating Targets", *IEEE Trans. GRS*, Vol. 48, Issue: 8, 2010.

[10] D. Pastina, F. Santi, M. Bucciarelli, P. Lombardo, "2D-MIMO SAR/ISAR imaging of moving targets with reconfigurable formation of platforms", Proc. of EUSAR 2012, Nuremberg (Germany), April 2012.

[11] D. Pastina, C. Spina, "Slope-based frame selection and scaling technique for ship ISAR imaging", IET Proc. on SP, Vol. 3, Issue 3, Sept.2008, pp. 265-276.

[12] M. Martorella, F. Berizzi, "Time Windowing for Highly Focused ISAR Image Reconstruction", IEEE Tr on Aerospace and Electronic Systems, Vol. 41, Issue 3, July 2005, Pages 992 – 1007.

[13] W. G. Carrara, R. S. Goodman, R. M. Majewski, "Spotlight Synthetic Aperture Radar", Artech House, Boston, 1995.

[14] M. Bucciarelli, D. Pastina "Distributed ISAR focusing for targets undergoing 3D motion", 2012 IET International Radar Conference, Glasgow (United Kingdom), October 2012.

[15] S. U. Pillai, B. Himed, K. Y. Li, "Orthogonal Pulsing Schemes for Improved Target Detection in Space Based Radar", 2005 IEEE Aerospace Conference, Big Sky, MT, March 5-12, 2005,

[16] S.U. Pillai, B. Himed, K.Y. Li, "Effect of Earth's rotation and range foldover on Space-based radar performance", IEEE Trans. AES, 2006, (42), (3), pp. 917-932.